

# Syntheses, crystal structures of a series of copper(II) complexes and their catalytic activities in the green oxidative coupling of 2,6-dimethylphenol

Erpeng Zhang<sup>a</sup>, Hongwei Hou<sup>a,b,\*</sup>, Huayun Han<sup>a</sup>, Yaoting Fan<sup>a</sup>

<sup>a</sup> Department of Chemistry, Zhengzhou University, Zhengzhou 450052, PR China

<sup>b</sup> State Key Laboratory of Coordination Chemistry, Nanjing University, Nanjing 210093, PR China

Received 18 December 2007; received in revised form 18 February 2008; accepted 21 February 2008

Available online 4 March 2008

## Abstract

Three mixed-ligand Cu<sup>II</sup> complexes bearing iminodiacetato (ida) and *N*-heterocyclic ligands, namely, [Cu<sub>2</sub>(ida)<sub>2</sub>(bbbm)(H<sub>2</sub>O)<sub>2</sub>] · H<sub>2</sub>O (**1**), [Cu<sub>2</sub>(ida)<sub>2</sub>(btx)(H<sub>2</sub>O)<sub>2</sub>] · 2H<sub>2</sub>O (**2**) and [Cu<sub>2</sub>(ida)<sub>2</sub>(pbbm)(H<sub>2</sub>O)<sub>2</sub>] · H<sub>2</sub>O · 3CH<sub>3</sub>OH (**3**) (bbbm = 1,1'-(1,4-butanediyl)bis-1*H*-benzimidazole, btx = 1,4-bis(1,2,4-triazol-1-ylmethyl)benzene, pbbm = 1,1'-(1,3-propanediyl)bis-1*H*-benzimidazole), in addition to three fcz-based Cu<sup>II</sup> complexes, namely, {[Cu(fcz)<sub>2</sub>(H<sub>2</sub>O)<sub>2</sub>] · 2NO<sub>3</sub>}<sub>n</sub> (**4**), {[Cu(fcz)<sub>2</sub>(H<sub>2</sub>O)] · SO<sub>4</sub> · DMF · 2CH<sub>3</sub>OH · 2H<sub>2</sub>O}<sub>n</sub> (**5**) and {[Cu(fcz)<sub>2</sub>Cl<sub>2</sub>] · 2CH<sub>3</sub>OH}<sub>n</sub> (**6**) (fcz = 1-(2,4-difluorophenyl)-1,1-bis[(1*H*-1,2,4-triazol-1-yl) methyl]ethanol) have been prepared according to appropriate synthetic strategies with the aim of exploiting new and potent catalysts. Single crystal X-ray diffraction shows that **1** and **2** possess similar binuclear structures, **3** features a 2D pleated network, and **4** exhibits a 1D polymeric double-chain structure. Complexes **1–6** are tested as catalysts in the green catalysis process of the oxidative coupling of 2,6-dimethylphenol (DMP). Under the optimized reaction conditions, these complexes are catalytically active by showing high conversion of DMP and high selectivity of PPE. The preliminary study of the catalytic–structural correlations suggests that the coordination environment of the copper center have important influences on their catalytic activities.

© 2008 Published by Elsevier B.V.

**Keywords:** Copper(II) complexes; Crystal structures; Green catalysis; Oxidative coupling; Catalytic–structural correlation

## 1. Introduction

Over a period of years, considerable efforts have been focused on the design and synthesis of the copper complex which attract extensive interests in many fields such as molecular magnetism [1], metalloproteins and enzymes [2]. In the specific case of catalysis, the unique characteristic of the Cu<sup>II</sup>/Cu<sup>I</sup> redox couple renders many of their complexes suited for various catalysis reactions [3], especially for the green catalysis process since copper is a cheap and minor toxic metal.

As a typical catalytic application of copper complexes, the oxidative coupling of 2,6-dimethylphenol (DMP) has received considerable attention [4–7] since the main product of this reaction, poly(1,4-phenylene ether) (PPE), is a valuable engineering plastic [8] with excellent mechanical properties and chemical resistance. Traditionally, the coupling reaction is carried out homogeneously in organic solvents or aqueous-organic biphasic solvents (in some cases) [9–12]. However, along with ever-growing environmental issues of chemical industry [13], the environmentally undesirable processes, wherever in the laboratory scale synthesis or in the manufacture of large-volume industrial chemicals, should be replaced by “greener” catalytic ones [14] with clean, safe, and inexpensive reaction solvents. Recently, Kei Saito and co-workers reported the oxidative coupling of DMP to form PPE with potassium ferricyanide as an

\* Corresponding author. Address: Department of Chemistry, Zhengzhou University, Zhengzhou 450052, PR China. Tel./fax: +86 371 67761744.

E-mail address: [houghw@zzu.edu.cn](mailto:houghw@zzu.edu.cn) (H. Hou).

oxidant in aqueous medium [15]. Unfortunately, the use of potassium ferricyanide is still environmentally deleterious. So far, the green oxidative coupling of DMP in environmental friendly solvents with clean oxidants is studied extremely rare. Therefore, this reaction is still a research field of great challenge from the standpoint of “green chemistry and technology”. Meantime, it is desired extraordinarily that the development of efficient copper-containing catalysts suited for the milder “green” conditions, and the investigation of catalytic–structural correlations which have great importance to exploiting new catalysts.

Hence, we prepared three mixed-ligand  $\text{Cu}^{\text{II}}$  complexes **1–3** and three fcz-based  $\text{Cu}^{\text{II}}$  complexes **4–6** according to appropriate synthetic strategies. For the purpose of replacing the traditional organic-medium systems by the environmental friendly processes, we explored an aqueous-medium catalysis process of the oxidative coupling of DMP by using hydrogen peroxide as oxidant and complexes **1–6** as catalysts. In order to understand the structural and chemical factors that govern the activities of catalysts, the catalytic–structural correlations have also been studied through examining the effects of coordination environment on the catalytic activities of the copper complexes.

## 2. Results and discussion

### 2.1. Synthesis

The self-assembly of  $\text{Cu}(\text{ida})$  building blocks and polydentate *N*-heterocyclic linkers has been proved to be a successful strategy in the construction of coordination polymeric frameworks [16]. According to this strategy, the reaction of  $\text{Cu}^{\text{II}}$  with *ida* ligand and *pbbm* linker in an aqueous-methanolic medium generated a 2D pleated network **3** as expected. With *bbbm* or *btx* as the linker, however, the corresponding product was binuclear complex **1** or **2** irrespective of the reasonable variation of pH or the reactants ratios. This suggests that the configuration and flexibility of the bridging ligands may be the determining factors for the structure of resulted complex. In addition, the presence of different counterions has important influence on the structure of cationic complex formed by neutral ligands. Formerly, we synthesized two fcz-based copper complexes by changing the counterions. With sulfate as the counterion, the 1D double chains coordination polymer **5** was obtained [17]. With chlorine as the counterion, the 2D network of complex **6** was formed [18]. Here, we chose nitrate as the counterion and synthesized a new 1D double chains coordination polymer **4** through the self-assembly of fcz ligand and copper ions.

### 2.2. Description of crystal structures

Crystallographic analysis reveals that complex  $[\text{Cu}_2(\text{ida})_2(\text{bbbm})(\text{H}_2\text{O})_2] \cdot \text{H}_2\text{O}$  (**1**) crystallizes in space group  $P\bar{1}$  and contains two kinds of crystallographically independent Cu ions (Cu1 and Cu2) as shown in Fig. 1. Around

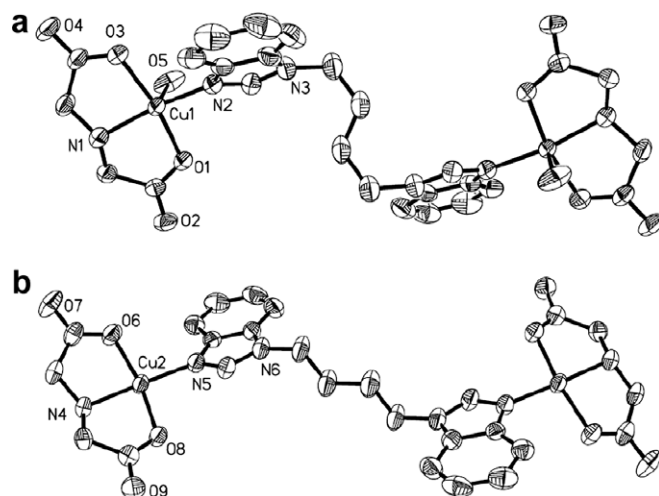


Fig. 1. ORTEP drawings of two independent molecules in complex **1** with thermal ellipsoids drawn at the 50% probability level. The hydrogen atoms and uncoordinated solvent molecules are omitted for clarity.

Cu1, the imino nitrogen N1 and two carboxylate oxygen atoms O1 and O3 from iminodiacetate take up the basal positions along with the nitrogen N2 of the bridging *bbbm* ligand, which lies across a crystallographic center of symmetry. An oxygen atom of coordinated water occupies the apical position, leading to a square pyramidal geometry around the Cu1 center. Unlike the Cu–N distances, the Cu–O distances here are disparate due to Jahn–Teller distortion of the  $\text{Cu}^{\text{II}}$  ion. The axial Cu1–O5 distance (2.392(3) Å) is much longer than the basal distances (1.965(3)–1.984(3) Å). The atoms N1, O1, O3 and N2 define a least-squares basal plane P(I), the Cu1 atom is displaced by 0.1259 Å from P(I) toward the apical oxygen atom O5. The benzimidazole plane P(II) of *bbbm* ligand defines a dihedral angle of 51.6° with P(I). Different from the five-coordinated Cu1, Cu2 is four-coordinated by *ida* and *bbbm* ligands. In the solid structure of **1**, the binuclear units are linked together through the hydrogen bonds formed by water molecules and carboxylate oxygen atoms of *ida* ligand, generating a 3D supramolecular structure as shown in Fig. 2.

Complex  $[\text{Cu}_2(\text{ida})_2(\text{btx})(\text{H}_2\text{O})_2] \cdot 2\text{H}_2\text{O}$  (**2**) crystallizes in space group  $P2_1/c$  with very similar structure to the Cu1 unit in **1**. As shown in Fig. 3, each Cu ion is located in the basal center of a square pyramidal geometry formed by the tridentate iminodiacetate, the bridging *btx* ligand and the coordinated water. Different from that in complex **1**, the dihedral angle between the basal plane P(I) (defined by the atoms N1, O1, O3, and N4) and the triazole plane P(II) of bridging *btx* ligand is 17.2°, which is comparable to those of  $[\text{Cu}(\text{ida})(\text{Meim})(\text{H}_2\text{O})_2] \cdot \text{H}_2\text{O}$  (Meim = *N*-methyl-imidazole) (16.3°) [19] and  $[\text{Cu}(\text{ida})(\text{im})(\text{H}_2\text{O})] \cdot \text{H}_2\text{O}$  (im = imidazole) (19.1°) [20]. As in **1**, the binuclear units of **2** are also linked together through intermolecular hydrogen bonds leading to a 3D network structure (Fig. 4).

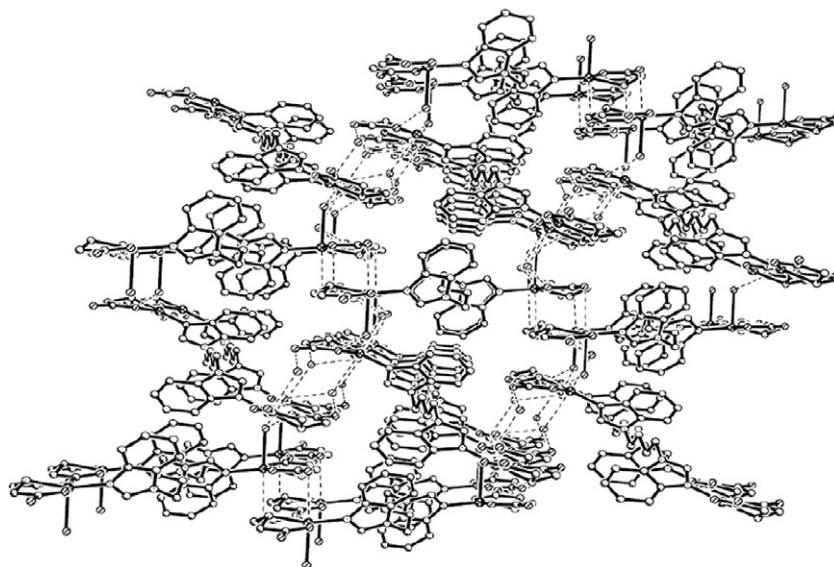


Fig. 2. View of the infinite 3D supramolecular structure of complex **1**, generated through extensive hydrogen bonding. The hydrogen atoms and uncoordinated water molecules are omitted for clarity.

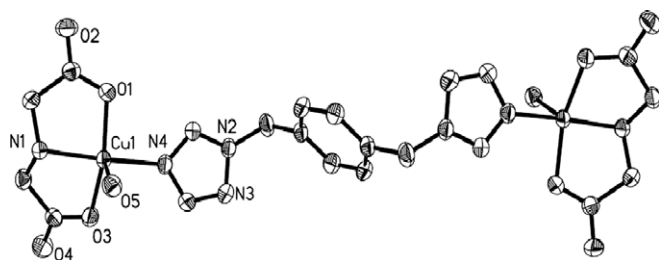


Fig. 3. ORTEP drawing of the binuclear structure of complex **2** with thermal ellipsoids drawn at the 50% probability level. The hydrogen atoms and uncoordinated water molecules are omitted for clarity.

Complex  $[\text{Cu}_2(\text{ida})_2(\text{pbbm})(\text{H}_2\text{O})_2] \cdot \text{H}_2\text{O} \cdot 3\text{CH}_3\text{OH}$  (**3**) is an extended 2D network crystallizing in space group  $P2_12_12_1$ . As in **1** and **2**, the atoms N1, O1 and O3 of the same iminodiacetate ligand and the N2 atom of the pbbm

molecule all coordinate to Cu1 forming a least-squares basal plane P(I) with the mean deviation of 0.0701 Å. Cu1 is displaced by 0.1602 Å from the plane P(I). Cu1 and Cu2 are bridged by the pbbm molecule leading to a binuclear  $[\text{Cu}_2(\text{ida})_2\text{pbbm}]$  unit (Fig. 5) which is similar to that of **1** or **2**. The dihedral angle between the benzimidazole plane P(II) of pbbm and P(I) ( $53.3^\circ$ ) is close to that of **1**. In addition, each  $\text{Cu}^{\text{II}}$  ion forms a somewhat longer bond (2.439(2) Å) to the fifth donor atom O4A of another  $[\text{Cu}_2(\text{ida})_2\text{pbbm}]$  unit, thus the square pyramidal coordination geometry around copper center is completed and two distinct carboxylate coordination modes of the same ida ligand are observed. The C1 carboxylate group is monodentate to Cu1 whereas the C4 carboxylate group forms a didentate bridge. As a consequence, these  $[\text{Cu}_2(\text{ida})_2\text{pbbm}]$  units are linked together through the longer Cu–O bonds leading to the infinite 2D pleated network

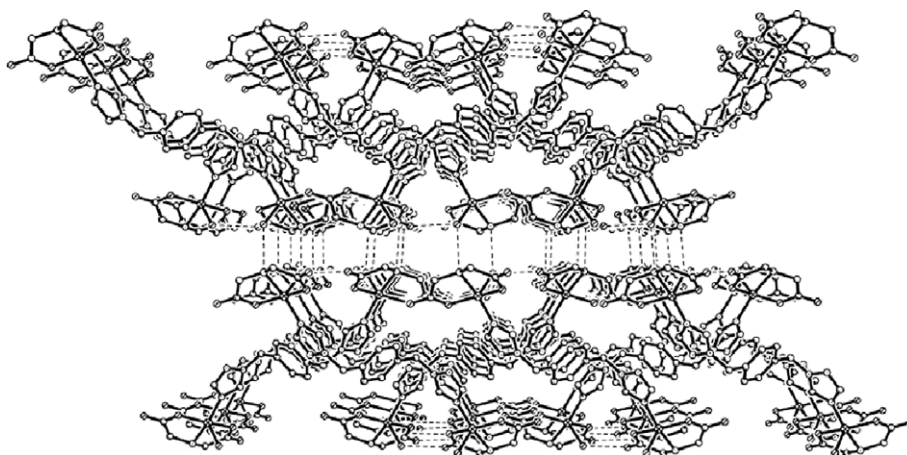


Fig. 4. View of the infinite 3D supramolecular structure of complex **2**, generated through extensive hydrogen bonding. The hydrogen atoms and uncoordinated water molecules are omitted for clarity.

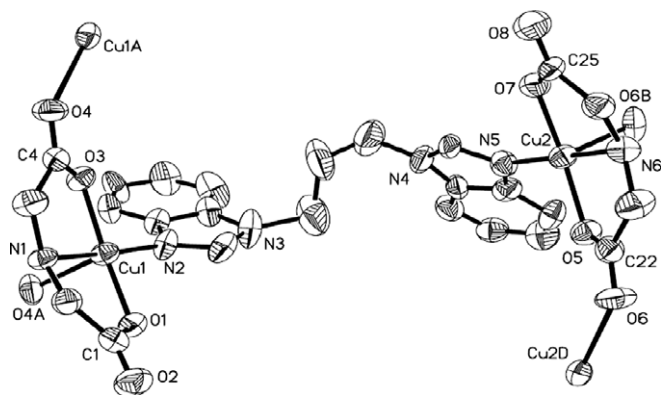


Fig. 5. The coordination environment of Cu ions of  $[\text{Cu}_2(\text{ida})_2(\text{pbbm})]$  group in complex **3** (ellipsoids at 50% probability). The hydrogen atoms and uncoordinated solvent molecules are omitted for clarity.

spread in *a* and *b* directions. As can be seen from Fig. 6, the individual ring of the network in **3** is made up of 6 Cu(ida) units connected together by two pbbm ligands leading to a puckered ring structure. Such 6-metallic rings also can be found in the reported mixed-ligand copper complexes [16], in which the honeycomb nets with interpenetrating frameworks are constructed by Cu(ida) units and bipyridine spacers.

Crystallographic analysis shows that complex  $\{[\text{Cu}(\text{fcz})_2(\text{H}_2\text{O})_2] \cdot 2\text{NO}_3\}_n$  (**4**) crystallizes in the triclinic space group *P* $\bar{1}$  and exhibits a 1D polymeric double-chain structure as shown in Fig. 7. Each  $\text{Cu}^{\text{II}}$  ion is located in the center of an elongated octahedron. Four nitrogen atoms from four fcz ligands occupy the equatorial sites, and two oxygen atoms from two coordinated water fill the axial positions. The Cu–O bond distance (2.3967(12) Å) is substantially longer than the basal Cu–N bond distances (2.0188(12)–2.0407(12) Å) due to Jahn–Teller distortion

of the  $\text{Cu}^{\text{II}}$  ion. The  $\text{Cu}^{\text{II}}$  ion locates strictly in the center of the equatorial plane P(I) (mean deviation = 0.0000 Å) defined by the atoms N1, N1A, N6B and N6C. Around the  $\text{Cu}^{\text{II}}$  ion, two triazole rings define the small dihedral angle of 21.1° with the equatorial plane P(I), which is comparable to the corresponding angle of complex **2**. But the other two triazole rings are nearly perpendicular to the equatorial plane with the dihedral angle of 88.4°. The fcz ligands link two  $\text{Cu}^{\text{II}}$  ions resulting in a bimetallic ring as building block. The bimetallic rings are extended through co- $\text{Cu}^{\text{II}}$  to generate an infinite double chain. As shown in Fig. 8, the nitrate anions are located in the vacancy among the 1D chains and hold the cationic chains together to generate a 2D layered architecture.

The crystal structures of complexes **5** and **6** have been described in our previous reports [17,18]. As shown in Scheme 1, complex **5** exhibits a 1D double-chain structure similar to that of complex **4**. Each  $\text{Cu}^{\text{II}}$  ion is located in the center of a distorted tetragonal pyramid. Four nitrogen atoms from four fcz ligands occupy the basal sites, and one oxygen atom from a terminally coordinated water molecule fills the apical position, which is different from that of complex **4**. Unlike **4** and **5**, complex **6** possesses a 2D rhombohedral grid structure, in which each copper center is 6-coordinated by two chlorine ions and four nitrogen atoms from four fcz ligands.

### 2.3. Catalytic oxidative coupling of DMP in water

The overall oxidative coupling process of DMP under green reaction conditions is shown in Scheme 2. The C–O coupling of DMP yields the linear polymer PPE, the C–C coupling and subsequent oxidation of two DMP units [21] result the by-product diphenoquinone (DPQ). Initially, we used complex **1** as a represent catalyst to optimize the

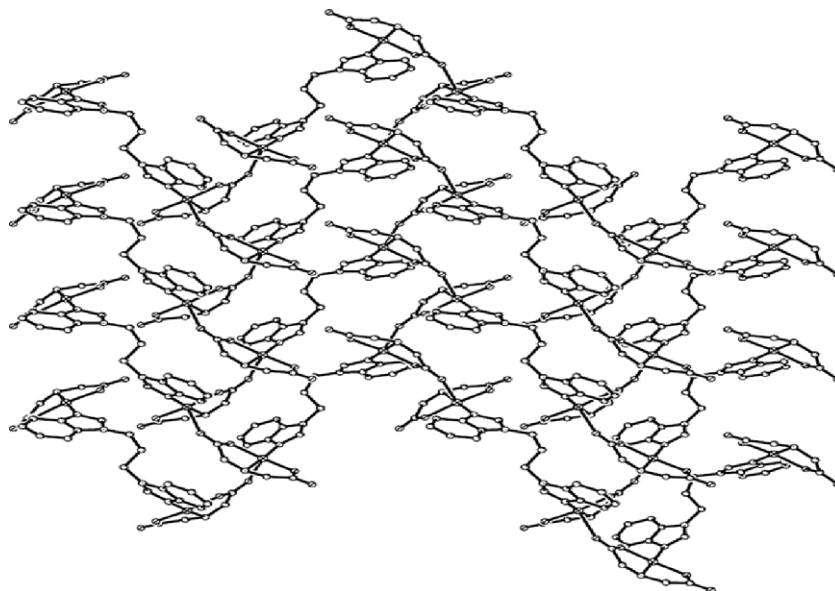


Fig. 6. View of the 2D pleated network involving 6-metallic rings. The hydrogen atoms and uncoordinated solvent molecules are omitted for clarity.

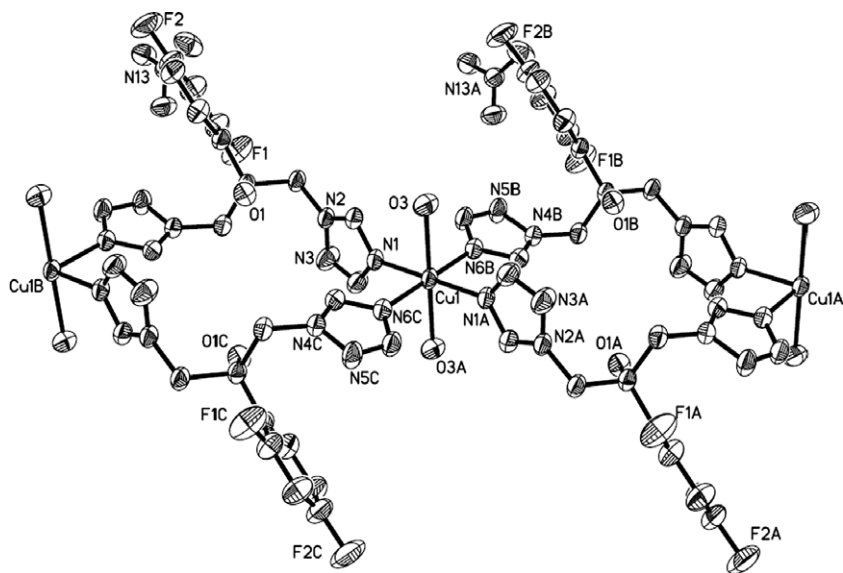


Fig. 7. The double-chain structure of complex 4. The hydrogen atoms are omitted for clarity.

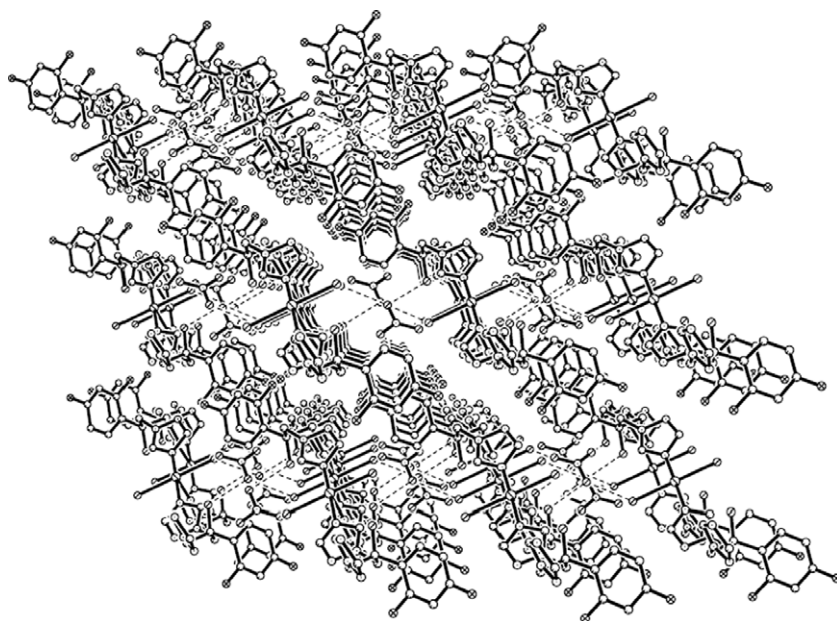


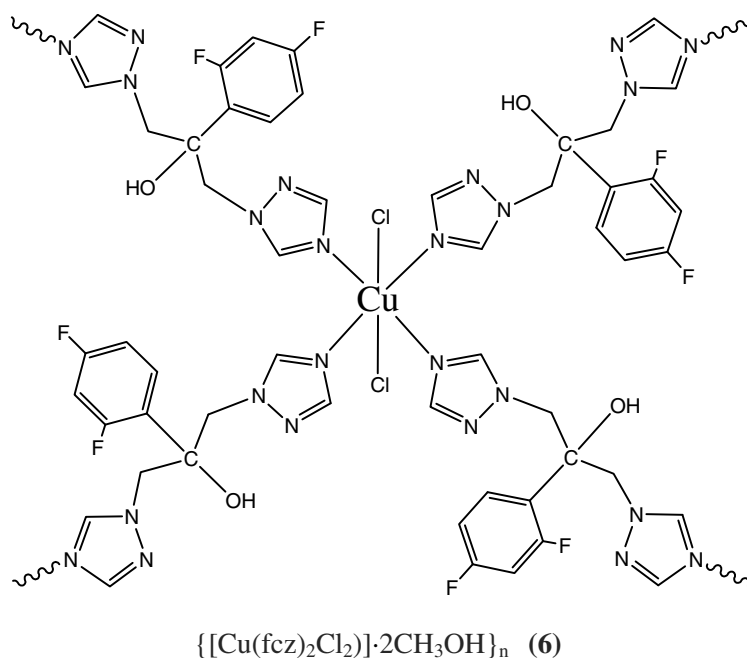
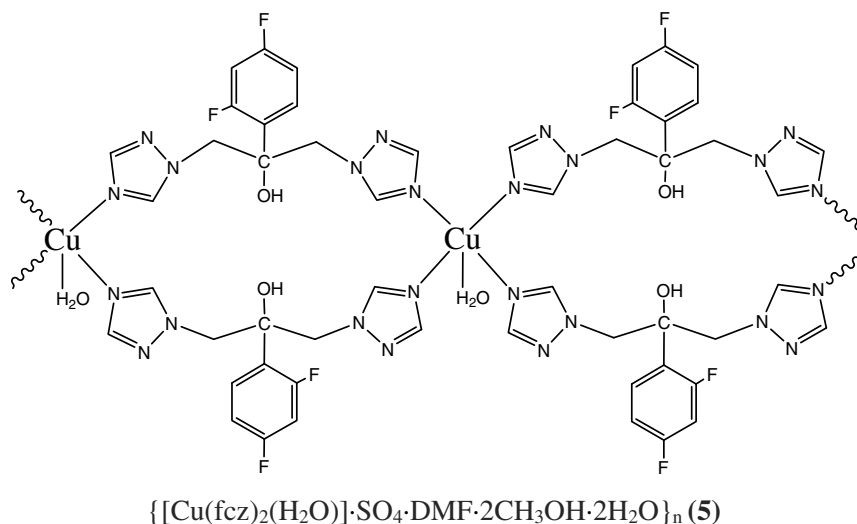
Fig. 8. The 2D supramolecular structure of complex 4, generated through extensive hydrogen bonding. The hydrogen atoms are omitted for clarity.

reaction conditions. As shown in Table 1, the influences of various factors such as reaction temperature, reaction time, the loading of catalyst, co-catalyst and oxidant were explored.

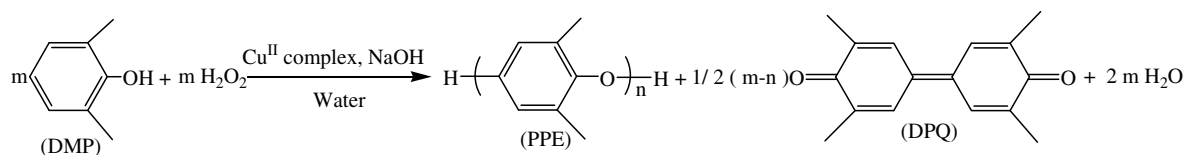
Previous investigations have indicated that the oxidative coupling of DMP in organic solvents is usually carried out at room temperature, and higher temperature will result in more by-products DPQ. However, as to the aqueous medium systems, higher temperature is necessary because the reaction does not proceed at room temperature (Entry 1). Thus several reaction temperatures (40, 50 and 60 °C) were screened (Entries 2–4). It is observed that a significant temperature effect on the reaction appeared. The DMP conver-

sion increases significantly from 77% to 93% as the temperature increases from 40 to 60 °C, and the best selectivity of PPE of 88% is achieved at the temperature of 50 °C.

The effect of reaction time was also investigated. As the time prolongs from 2 h to 8 h, the DMP conversion increases quickly from about 50% to near 90%, while the selectivity of PPE increases very slowly. Further prolonging in reaction time does not improve the conversion significantly but decreases the selectivity slightly (Entry 8). The reason for this may be that the by-product DPQ degrades the polymer upon further processing at high temperatures [22]. In addition, we find that the selectivity of PPE is not



Scheme 1. The structures of complexes 5 and 6.



Scheme 2. The oxidative coupling of 2,6-dimethylphenol in water.

correlated for the DMP conversion, which is closely to the former conclusion [22], since Viersen et al. have shown that most DPQ is formed during the beginning of the reaction [23].

It has been demonstrated that this coupling process does not proceed without the addition of base [15]. The role of base is considered to be deprotonation of DMP into phenolate species, which is crucial in the whole catalytic pro-

cess [4]. Thus, the effect of various NaOH-to-DMP ratios on the reaction was surveyed (Entries 13–16). It is clear that the DMP conversion increases dramatically with the increase of NaOH-to-DMP ratio. The favorable effect on the selectivity reaches the maximum of 88% at a 1:1 ratio of NaOH-to-DMP. But the excess amount of NaOH results in a decrease of the selectivity although the substrates convert more completely (Entry 16). The aforemen-

Table 1  
Oxidative coupling of DMP in water catalyzed by complex **1**

Entry	Temperature (°C)	Time (h)	Complex <b>1</b> (mol%)	NaOH/DMP	H <sub>2</sub> O <sub>2</sub> (μL)	Conversion <sup>a</sup> (%)	Selectivity <sup>b</sup> (%)
1	RT	8	2	1	30	NR	
2	40	8	2	1	30	77	69
3	50	8	2	1	30	89	88
4	60	8	2	1	30	93	83
5	50	2	2	1	30	52	80
6	50	6	2	1	30	76	86
7	50	8	2	1	30	89	88
8	50	12	2	1	30	96	83
9	50	8	0	1	30	Trace	
10	50	8	1	1	30	80	81
11	50	8	2	1	30	89	88
12	50	8	4	1	30	90	89
13	50	8	2	0.5	30	80	77
14	50	8	2	0.8	30	84	86
15	50	8	2	1	30	89	88
16	50	8	2	1.2	30	94	85
17	50	8	2	1	0	76	81
18	50	8	2	1	10	85	85
19	50	8	2	1	20	88	88
20	50	8	2	1	30	89	88
21	50	8	2	1	40	98	82

<sup>a</sup> Conversions and isolated yields based on the DMP, average of two runs.

<sup>b</sup> Selectivity =  $([\text{PPE}] \times 100)/([\text{PPE}] + [\text{DPQ}])$ .

Table 2  
Oxidative coupling of DMP catalyzed by complexes **1–6**<sup>a</sup>

Catalysts	Conversion (%) <sup>b</sup>	Yield (%) <sup>b</sup>		Selectivity (%) <sup>c</sup>	PPE	
		PPE	DPQ		<i>M<sub>w</sub></i> (/10 <sup>3</sup> )	<i>M<sub>w</sub></i> / <i>M<sub>n</sub></i>
1	88	69	9	88	10.5	2.0
2	77	60	11	84	9.6	1.8
3	83	74	8	90	11.3	2.1
CuCl <sub>2</sub>	Trace					
4	82	46	9	84	6.2	1.7
5	86	45	7	86	7.1	1.6
6	73	50	8	86	4.5	1.3

<sup>a</sup> Optimized conditions: DMP (1 mmol), NaOH (1 mmol), H<sub>2</sub>O<sub>2</sub> (20 μL) and catalyst (0.02 mmol) in 5 mL of water for 8 h at 50 °C.

<sup>b</sup> Conversions and isolated yields based on the DMP, average of two runs.

<sup>c</sup> Selectivity =  $([\text{PPE}] \times 100)/([\text{PPE}] + [\text{DPQ}])$ .

tioned data, taken together with the previous finding of a competing effect of hydroxide ions with phenolate anions induced by the excess of basicity [24], allow a 1:1 ratio of NaOH-to-DMP for optimization.

The influences of the loading of catalyst and oxidant have also been explored. The control reaction performed without any catalyst (Entry 9) shows that the copper complex is indispensable for the reaction system. But the effect of the amounts of catalyst is not striking and 2 mol% of complex **1** is sufficient. The results of entries 17–21 indicate that the addition of appropriate amount of H<sub>2</sub>O<sub>2</sub> is also necessary for obtaining higher conversion and selectivity. At higher amounts of H<sub>2</sub>O<sub>2</sub>, the substrates almost convert completely but the selectivity descends correspondingly. Similar results have been found in our previous investigations [25].

After acquiring the optimized reaction conditions for complex **1**, the other two mixed-ligand complexes **2** and **3**

were also tested as catalysts for this oxidative coupling reaction under the same conditions. As shown in Table 2, complex **3** provides the results similar to that of **1** with 83% conversion and 90% selectivity. The performance of complex **2** is slightly poorer than the above two catalysts giving 77% conversion and 84% selectivity. Comparing with the [Cu(tmeda)Cl<sub>2</sub>] catalyst giving 67% yield of PPE [15], the best result of the copper-catalyzed synthesis of PPE in aqueous medium so far, complexes **1** and **3** are more efficient catalysts with the yields of PPE of 69% for **1** and 74% for **3**, respectively. However, the contrasting reaction using CuCl<sub>2</sub> as catalyst only gives trace amounts of PPE. We also notice that the Cu(NO<sub>3</sub>)<sub>2</sub>/Meim catalyst which has been used successfully in organic systems, shows a poor result in water with nearly no PPE obtained [12]. This suggests that complexes **1–3** have obvious comparative advantage in the aqueous-medium oxidative coupling

of DMP. A potential explanation for this may be inferred from the stabilizing effects [17,25] of the ida ligand and the steric influence of the copper center. In case of complexes 1–3, the tridentate mode of ida ligand not only improves the aqueous stabilities of these complexes but also forms the opening coordination geometry with less steric hindrance around the copper center which favors the coordination of DMP to Cu<sup>II</sup> to form the proposed active copper species [26] and the subsequent polymerization of DMP. Likewise, Reedijk and co-workers have also shown that a series of Cu<sup>II</sup> complexes incorporating structurally related *N,O*-containing ligands underwent this polymerization more efficiently than copper(II) salts [7d]. As to the slightly lower DMP conversion obtained by complex 2, the possible reason may associate with the features of different *N*-heterocyclic ligands presented in these complexes.

In order to further elucidate the influence of the coordination environment on the catalytic activities of copper complexes, and understand the structural and chemical factors that govern the activities of catalysts in aqueous systems, three fcz-based complexes 4–6 with different coordination geometries were studied as catalysts for the oxidative coupling of DMP, the results were also reported in Table 2. Under the same reaction conditions, complexes 4 and 5 with one or two coordinated water molecules around each copper center give similar results with the conversion of 86% and 82%, respectively. As premeditated, complex 6 with coordinated chloride ions is found to be the least active catalyst with only 73% conversion. Although no remarkable differences exist among the conversions obtained by complexes 4–6, these results, to a certain extent, represent the influence of the coordination environment on the catalytic activity of the copper complex. Concretely, comparing with the strongly coordinated chloride ions in complex 6, the coordinated water molecules in 4 and 5 are easy leaving groups and can be readily replaced by the oxidant or the substrate, thus it is easier, for the phenolate anion, to enter the copper coordination sphere when copper centers are coordinated by water molecules rather than chloride ions.

On the basis of the above experimental results and previous literatures [4–7,15], we propose a plausible reaction mechanism for the present oxidative coupling reaction. DMP is dissolved in the basic aqueous phase to form the phenolate anion; these phenolate anions coordinate to the Cu<sup>II</sup> center and subsequently are oxidized by Cu<sup>II</sup> to the phenoxyl radicals [15]. The C–O coupling of these phenoxyl radicals gives the polymer in the solid that precipitates from the water. The resultant Cu<sup>I</sup> was reoxidized to Cu<sup>II</sup> by H<sub>2</sub>O<sub>2</sub>.

Although the optimal yields obtained by these complexes in water are not high (45–74%) comparing with those results obtained from organic systems, the present system has the following significant advantages from the standpoint of “green chemistry and technology”: (i) hydrogen peroxide and water are used to replace the environmental unfriendly oxidants and reaction solvents, (ii) the use of

mixed-ligand copper complexes catalysts may represent a starting point for the development of new kinds of catalysts satisfying the need of “green” process.

### 3. Conclusion

In summary, with the aim of exploiting new and potent catalysts, we have synthesized three mixed-ligand complexes 1–3 by the self-assembly of Cu(ida) building block with different auxiliary ligands, and three fcz-based complex 4–6 by the self-assembly of Cu<sup>II</sup> ions with fcz ligand in the presence of different counterions. Using complexes 1–6 as catalysts, a green aqueous-medium catalysis process of the oxidative coupling of DMP has been explored with great potentials in the aspect of “green chemistry and technology”. Recognizing that decreasing the steric hindrance around the copper center should increase the catalytic activity of complex, it can be expected that more studies could improve the catalytic efficiencies via further structural modifications of copper complex for practical application.

### 4. Experimental

#### 4.1. General

All reagents were obtained from commercial suppliers and used without further purification. 2,6-dimethylphenol (DMP) (99% pure) was used as obtained from J&K Chemical Ltd. IR data were recorded on a Bruker Tensor 27 spectrophotometer with KBr pellets in the 400–4000 cm<sup>-1</sup> region. NMR spectra were recorded on a Bruker DPX-400 spectrometer. Elemental analyses (C, H, and N) were carried out on a FLASH EA 1112 elemental analyzer. Molecular weights of the PPE were determined on a Waters 150C gel permeation chromatography (GPC) instrument. Polystyrene was used as calibration standards. THF was used as an eluent at a flow rate of 1.0 ml/min.

Ligand 1,4-bis(1,2,4-triazol-1-ylmethyl)benzene (btz) was prepared according to our previous procedures [27]. Ligands 1,1'-(1,3-propanediyl)bis-1*H*-benzimidazole (pbbm) and 1,1'-(1,4-butanediyl)bis-1*H*-benzimidazole (bbbm) were prepared according to the literature [28], except that benzimidazole was used instead of benzotriazole.

#### 4.2. Synthesis of complex 1–6

*Synthesis of [Cu<sub>2</sub>(ida)<sub>2</sub>(bbbm)(H<sub>2</sub>O)<sub>2</sub>] · H<sub>2</sub>O (1):* An aqueous solution (2 mL) of sodium iminodiacetate (8.8 mg, 0.05 mmol) was added into the 3 mL methanol solution of CuCl<sub>2</sub> · 2H<sub>2</sub>O (8.5 mg, 0.05 mmol), then 3 mL methanol solution of bbbm (7.2 mg, 0.025 mmol) was added drop wise to the above mixture. The resulting dark blue solution was allowed to stand at room temperature. After a few days, blue block-shaped crystals of complex 1 were obtained. The solid were collected by filtration and dried in vacuo. The sample is stable in the air. Yield:



66%. IR ( $\text{cm}^{-1}$ , KBr): 3387 s, 3255 m, 2945 w, 1623 s, 1522 m, 1467 w, 1393 s, 1300 m, 1262 w, 1202 m, 1121 w, 1015 w, 910 m, 750 s. Anal. Calc. for  $\text{C}_{26}\text{H}_{32}\text{Cu}_2\text{N}_6\text{O}_{11}$ : C, 42.68; H, 4.41; N, 11.49. Found: C, 43.02; H, 4.13; N, 11.38%.

**Synthesis of  $[\text{Cu}_2(\text{ida})_2(\text{btx})(\text{H}_2\text{O})] \cdot 2\text{H}_2\text{O}$  (**2**):** The procedure was similar to that of **1**, except that btx was used instead of bbbm. The resulting dark blue solution was allowed to stand at room temperature. After a few days, blue block-shaped crystals of complex **2** were obtained. The solid were collected by filtration and dried in vacuo. The sample is stable in the air. Yield: 69%. IR ( $\text{cm}^{-1}$ , KBr): 3238 s, 3137 s, 1620 s, 1536 m, 1442 m, 1389 s, 1301 m, 1131 s, 1006 m, 914 m, 738 m. Anal. Calc. for  $\text{C}_{20}\text{H}_{27}\text{Cu}_2\text{N}_8\text{O}_{12}$ : C, 34.49; H, 3.90; N, 16.04. Found: C, 34.76; H, 3.69; N, 16.30%.

**Synthesis of  $[\text{Cu}(\text{ida})_2(\text{pbbm})(\text{H}_2\text{O})_2] \cdot 2\text{H}_2\text{O}$  (**3**):** The procedure was also similar to that of **1**, except that pbbm was used instead of bbbm. The resulting dark blue solution was allowed to stand at room temperature. A few weeks later, blue block-shaped crystals of complex **3** had deposited. The solid were collected by filtration and dried in vacuo. The sample is stable in the air. Yield: 53%. IR ( $\text{cm}^{-1}$ , KBr): 3372 m, 3139 m, 1611 s, 1510 m, 1461 w, 1384 s, 1259 w, 1193 m, 1124 w, 1021 w, 908 m, 757 m. Anal. Calc. for  $\text{C}_{28}\text{H}_{44}\text{Cu}_2\text{N}_6\text{O}_{14}$ : C, 41.22; H, 5.44; N, 10.30. Found: C, 41.60; H, 5.06; N, 10.25%.

**Synthesis of  $\{[\text{Cu}(\text{fcz})_2(\text{H}_2\text{O})_2] \cdot 2\text{NO}_3\}_n$  (**4**):** A methanol solution (3 mL) of fcz (0.2 mmol) was slowly added into 3 mL methanol solution of  $\text{Cu}(\text{NO}_3)_2 \cdot 3\text{H}_2\text{O}$  (0.1 mmol). The resulting azury solution was allowed to stand at room temperature. A few weeks later, blue block-shaped crystals of complex **4** had deposited. The solid were collected by filtration and dried in vacuo. The sample is stable in the air. Yield: 50%. IR ( $\text{cm}^{-1}$ , KBr): 3439 s, 3130 s, 1620 s, 1503 m, 1277 m, 1132 s, 676 m. Anal. Calc. for  $\text{C}_{26}\text{H}_{28}\text{CuF}_4\text{N}_{14}\text{O}_{10}$ : C, 37.31; H, 3.35; N, 23.44. Found: C, 37.35; H, 3.39; N, 23.49%.

**Synthesis of  $\{[\text{Cu}(\text{fcz})_2(\text{H}_2\text{O})] \cdot \text{SO}_4 \cdot \text{DMF} \cdot 2\text{CH}_3\text{OH} \cdot 2\text{H}_2\text{O}\}_n$  (**5**):** Complex **5** was synthesized according to our previous procedure [17]. A mixture of methanol and DMF solution (6 mL) of fcz (0.2 mmol) was slowly added into 1 mL aqueous solution of  $\text{CuSO}_4 \cdot 5\text{H}_2\text{O}$  (0.1 mmol). The resulting clear solution was allowed to stand at room temperature. A few weeks later, blue block-shaped crystals of complex **5** were formed. The solid were collected by filtration and dried in vacuo. The sample is stable in the air. Yield: 58%. IR ( $\text{cm}^{-1}$ , KBr): 3445 s, 3131 s, 1620 s, 1500 m, 1279 m, 1130 s, 675 m. Anal. Calc. for  $\text{C}_{31}\text{H}_{45}\text{CuF}_4\text{N}_{13}\text{O}_{12}\text{S}$ : C, 38.61; H, 4.67; N, 18.89. Found: C, 38.52; H, 4.67; N, 18.76%.

**Synthesis of  $\{[\text{Cu}(\text{fcz})_2\text{Cl}_2] \cdot 2\text{CH}_3\text{OH}\}_n$  (**6**):** Complex **6** was synthesized according to the literature [18]. The procedure was similar to that of **4**, except that  $\text{CuCl}_2 \cdot 2\text{H}_2\text{O}$  was used instead of  $\text{Cu}(\text{NO}_3)_2 \cdot 3\text{H}_2\text{O}$ . The azury block-shaped crystals of complex **6** are also stable in the air. Yield: 63%. IR ( $\text{cm}^{-1}$ , KBr): 3448 s, 3132 s, 1619 s, 1501 s, 1278 s,

992 m, 673 m. Anal. Calc. for  $\text{C}_{28}\text{H}_{32}\text{CuCl}_2\text{F}_4\text{N}_{12}\text{O}_4$ : C, 41.43; H, 3.95; N, 20.72. Found: C, 41.49; H, 3.90; N, 20.74%.

#### 4.3. General procedure for the catalytic oxidative coupling of 2,6-dimethylphenol

All of the crystal complex catalysts were ground well into appropriate sizes prior to use. DMP (122 mg, 1 mmol) was dissolved in water (5 mL) containing sodium hydroxide (40 mg, 1 mmol) and sodium *n*-dodecyl sulfate (SDS) (29 mg, 0.1 mmol) in a 10 mL flask. The 2 mol% complex was added to the solution, and the mixture was vigorously stirred under air at 50 °C. Then, hydrogen peroxide (30% aqueous solution) was slowly added into the mixture using a microinjector every 15 min for 2 times to minimize  $\text{H}_2\text{O}_2$  decomposition. After 8 h, the reaction was stopped and the polymer product appeared as an off-white powder after salting out by the addition of sodium chloride (1.17 g, 0.02 mol). Then the mixture was transferred into a separatory funnel, the organic materials were extracted after the addition of a few milliliters of  $\text{CH}_2\text{Cl}_2$ . This was repeated 3 times. The combined organic extracts were dried with anhydrous  $\text{MgSO}_4$  and the solvent, after filtration, was evaporated in vacuo. The products were separated by preparative TLC performed on dry silica gel plates with ethyl ether–petroleum ether (1:3 v/v) as the developing solvents. PPE and DPQ were collected and dried in vacuo. We also can get the polymeric products by the simple filtration after salting out, followed by the reprecipitation from chloroform to methanol.

**Poly(phenylene ether) (PPE):**  $^1\text{H}$  NMR (400 MHz,  $\text{CDCl}_3$ )  $\delta$ : 2.10 (s, 6H), 6.45 (s, 2H).  $^{13}\text{C}$  NMR (100 MHz,  $\text{CDCl}_3$ )  $\delta$ : 16.8, 114.5, 132.7, 145.6, 154.5. IR ( $\text{cm}^{-1}$ , KBr): 3429 m, 1607 s, 1471 s, 1306 s, 1189 s, 1022 s, 858 m.

#### 4.4. X-ray crystallographic analyses

The data of **1** and **4** were collected on a Bruker ApeX CCD diffractometer with graphite monochromated  $\text{Mo K}\alpha$  radiation ( $\lambda = 0.71073 \text{ \AA}$ ). The data of **2** and **3** were collected on a Rigaku Saturn 724 CCD diffractometer with graphite monochromated  $\text{Mo K}\alpha$  radiation ( $\lambda = 0.71073 \text{ \AA}$ ). A single crystal suitable for X-ray diffraction was mounted on a glass fiber. The data were collected at room temperature and corrected for Lorentz-polarization effects. A correction for secondary extinction was applied. The structures were solved by direct methods and expanded using Fourier techniques. The non-hydrogen atoms were refined anisotropically and hydrogen atoms were included but not refined. The final cycle of full-matrix least-squares refinement was based on observed reflections and variable parameters. All calculations were performed using the SHELXL-97 crystallographic software package [29], and refined by full-matrix least squares methods based on  $F^2$  with isotropic thermal parameters for the non-hydrogen atoms. Table 3

Table 3  
Crystal data and structure refinement for complexes 1–4

Complex	1	2	3	4
Formula	C <sub>26</sub> H <sub>32</sub> Cu <sub>2</sub> N <sub>6</sub> O <sub>11</sub>	C <sub>20</sub> H <sub>30</sub> Cu <sub>2</sub> N <sub>8</sub> O <sub>12</sub>	C <sub>28</sub> H <sub>44</sub> Cu <sub>2</sub> N <sub>6</sub> O <sub>14</sub>	C <sub>26</sub> H <sub>28</sub> CuF <sub>4</sub> N <sub>14</sub> O <sub>10</sub>
<i>F</i> <sub>w</sub>	731.66	701.60	815.77	836.16
<i>T</i> (K)	291(2)	293(2)	293(2)	293(2)
Wavelength (Å)	0.71073	0.71073	0.71073	0.71073
Crystal system	Triclinic	Monoclinic	Orthorhombic	Triclinic
Space group	<i>P</i> $\bar{1}$	<i>P</i> 2 <sub>1</sub> / <i>c</i>	<i>p</i> 2 <sub>1</sub> 2 <sub>1</sub>	<i>P</i> $\bar{1}$
<i>a</i> (Å)	10.0069(19)	13.849(3)	8.0276(16)	9.4225(7)
<i>b</i> (Å)	12.048(2)	11.039(2)	19.859(4)	10.4660(8)
<i>c</i> (Å)	13.382(3)	9.4429(19)	21.265(4)	10.7979(8)
$\alpha$ (°)	89.099(4)	90	90	62.2480(10)
$\beta$ (°)	87.413(4)	104.24(3)	90	72.9370(10)
$\gamma$ (°)	68.766(4)	90	90	69.8560(10)
<i>V</i> (Å <sup>3</sup> )	1502.3(5)	1399.2(5)	3390.1(12)	873.29(11)
<i>Z</i> , <i>D</i> <sub>c</sub> (g cm <sup>-3</sup> )	2, 1.617	2, 1.665	4, 1.492	1, 1.590
<i>F</i> (000)	752	720	1572	427
$\theta$ Range for data collection (°)	2.37–27.50	1.52–28.07	1.92–24.99	2.27–27.50
Reflection collected/unique ( <i>R</i> <sub>int</sub> )	13014/6767 (0.0187)	16916/3376 (0.0568)	33673/5972 (0.0473)	7651/3947 (0.0108)
Data/restraints/parameters	6767/9/430	3376/2/202	5972/0/442	3947/0/250
Goodness-of-fit on <i>F</i> <sup>2</sup>	1.019	1.050	1.094	0.954
Final <i>R</i> <sub>1</sub> , <sup>a</sup> <i>wR</i> <sub>2</sub> <sup>b</sup>	0.0395, 0.0991	0.0396, 0.0972	0.0782, 0.2272	0.0299, 0.1072

<sup>a</sup>  $R1 = \sum ||F_o| - |F_c|| / \sum |F_o|$ .

<sup>b</sup>  $wR2 = [\sum w(|F_o|^2 - |F_c|^2)|^2 / \sum w|F_o|^2]^{1/2}$ ,  $w = 1/[\sigma^2(F_o)^2 + 0.0297P^2 + 27.5680P]$ , where  $P = (F_o^2 + 2F_c^2)/3$ .

Table 4  
Selected bond lengths (Å) and angles (°) for complexes 1–4

Complex 1							
Cu1–O1	1.9653(19)	Cu1–O3	1.965(2)	Cu1–O5	2.392(3)	Cu1–N1	1.984(3)
Cu1–N2	1.941(2)	Cu2–O8	1.975(2)	Cu2–O6	1.970(2)	Cu2–N4	1.993(2)
Cu2–N5	1.962(2)	O1–Cu1–O3	167.33(9)	N1–Cu1–N2	161.99(11)	O6–Cu2–O8	165.74(9)
N4–Cu2–N5	177.49(10)	O5–Cu1–O1	85.32(9)	O5–Cu1–N1	101.08(11)	O5–Cu1–O3	91.93(9)
O5–Cu1–N2	96.68(11)						
Complex 2							
Cu1–O1	1.9533(18)	Cu1–O3	1.9518(18)	Cu1–O5	2.257(2)	Cu1–N1	1.968(2)
Cu1–N4	1.9593(19)	N1–Cu1–N4	167.73(8)	O1–Cu1–O3	161.01(8)	O5–Cu1–N1	98.87(8)
O5–Cu1–N4	93.39(8)	O5–Cu1–O1	96.93(9)	O5–Cu1–O3	100.43(8)		
Complex 3 <sup>a</sup>							
Cu1–O1	1.974(5)	Cu1–O3	1.990(5)	Cu1–O4#1	2.439(6)	Cu1–N1	1.985(6)
Cu1–N2	1.964(6)	Cu2–O5	2.001(5)	Cu2–O7	1.974(5)	Cu2–O6#2	2.386(6)
Cu2–N6	1.997(6)	Cu2–N5	1.962(6)	N1–Cu1–N2	174.3(3)	O1–Cu1–O3	163.0(2)
N5–Cu2–N6	175.5(3)	O5–Cu2–O7	162.4(2)	O4#1–Cu1–N1	90.2(2)	O4#1–Cu1–N2	95.2(2)
O4#1–Cu1–O1	93.3(2)	O4#1–Cu1–O3	99.6(2)				
Complex 4 <sup>b</sup>							
Cu1–N1	2.0188(12)	Cu1–N1#1	2.0188(12)	Cu1–N6#2	2.0407(12)	Cu1–N6#3	2.0407(12)
Cu1–O3	2.3967(12)	Cu1–O3#1	2.3967(12)	N1–Cu1–N1#1	180.000(1)	N6#2–Cu1–N6#3	180.00(8)
O3–Cu1–O3#1	180.000(1)	O3–Cu1–N1	93.37(5)	N1–Cu1–O3#1	86.63(5)		

<sup>a</sup> Symmetry transformations used to generate equivalent atoms: #1  $x - 1/2, -y + 3/2, -z + 2$ , #2  $x + 1/2, -y + 1/2, -z + 2$ .

<sup>b</sup> Symmetry transformations used to generate equivalent atoms: #1  $-x + 1, -y + 1, -z + 2$ , #2  $-x + 1, -y, -z + 2$ , #3  $x, y + 1$ .

shows crystallographic data and structure processing parameters of complexes 1–4. Selected bond lengths and bond angles of complexes 1–4 are listed in Table 4.

#### Acknowledgement

We thank the National Natural Science Foundation (Nos. 20671082 and 20371042), NCET and Ph.D. Foundation of Ministry of Education of China for financial support.

#### Appendix A. Supplementary material

CCDC 666231, 666232, 666233, and 666234 contain the supplementary crystallographic data for this paper. These data can be obtained free of charge from The Cambridge Crystallographic Data Centre via [www.ccdc.cam.ac.uk/data\\_request/cif](http://www.ccdc.cam.ac.uk/data_request/cif). Supplementary data associated with this article can be found, in the online version, at [doi:10.1016/j.jorganchem.2008.02.023](https://doi.org/10.1016/j.jorganchem.2008.02.023).

## References

- [1] J. Mroziński, *Coord. Chem. Rev.* 249 (2005) 2534.
- [2] (a) L.M. Mirica, X. Ottenwaelder, T.D.P. Stack, *Chem. Rev.* 104 (2004) 1013;  
(b) E.A. Lewis, W.B. Tolman, *Chem. Rev.* 104 (2004) 1047;  
(c) S.J. Elliott, M. Zhu, L. Tso, H.H.T. Nguyen, J.H.K. Yip, S.I. Chan, *J. Am. Chem. Soc.* 119 (1997) 9949.
- [3] (a) S. Hattori, I. Noguchi, *Nature* 184 (1959) 1145;  
(b) J.W. Godden, S. Turley, D.C. Teller, E.T. Adman, M.Y. Liu, W.J. Payne, J. LeGall, *Science* 253 (1991) 438;  
(c) N. Kitajima, *Adv. Inorg. Chem.* 39 (1992) 1;  
(d) T.N. Sorrell, *Tetrahedron* 45 (1989) 3;  
(e) J.P. Klinman, *Chem. Rev.* 96 (1996) 2541.
- [4] (a) A.S. Hay, H.S. Blanchard, G.F. Endres, J.W. Eustance, *J. Am. Chem. Soc.* 81 (1959) 6335;  
(b) E. Tsuchida, M. Kaneko, H. Nishide, *Makromol. Chem.* 151 (1972) 221;  
(c) E. Tsuchida, H. Nishide, *Makromol. Chem.* 176 (1975) 1349;  
(d) E. Tsuchida, H. Nishide, *Adv. Polym. Sci.* 24 (1977) 1;  
(e) G.D. Cooper, H.S. Blanchard, G.F. Endres, H. Finkbeiner, *J. Am. Chem. Soc.* 87 (1965) 3996;  
(f) J. Kresta, A. Tkac, R. Prikryl, L. Malik, *Makromol. Chem.* 176 (1975) 157.
- [5] (a) A. Camus, M.S. Garozzo, N. Marsich, M. Mari, *J. Mol. Catal. A* 112 (1996) 353;  
(b) P.J. Baesjou, W.L. Driessen, G. Challa, J. Reedijk, *J. Mol. Catal. A* 135 (1998) 273;  
(c) P.J. Baesjou, W.L. Driessen, G. Challa, J. Reedijk, *J. Mol. Catal. A* 140 (1999) 241;  
(d) P.J. Baesjou, W.L. Driessen, G. Challa, J. Reedijk, *Macromolecules* 32 (1999) 270.
- [6] (a) W. Koch, W. Risse, W. Heitz, *Makromol. Chem. Suppl.* 12 (1985) 105;  
(b) E. Tsuchida, F. Suzuki, E. Shouji, K. Yamamoto, *Macromolecules* 27 (1994) 1057;  
(c) P.J. Baesjou, W.L. Driessen, G. Challa, J. Reedijk, *J. Am. Chem. Soc.* 119 (1997) 12590;  
(d) H.A.M. van Aert, M.H.P. van Gendersen, G.J.M.L. van Steenpaal, L. Nelissen, E.W. Meijer, J. Liska, *Macromolecules* 30 (1997) 6056;  
(e) H. Higashimura, K. Fujisawa, Y. Moro-oka, M. Kubota, A. Shiga, A. Terahara, H. Uyama, S. Kobayashi, *J. Am. Chem. Soc.* 120 (1998) 8529.
- [7] (a) K. Oyaizu, Y. Kumaki, K. Saito, E. Tsuchida, *Macromolecules* 33 (2000) 5766;  
(b) J. Gao, J.H. Reibenspies, A.E. Martell, *Inorg. Chim. Acta* 338 (2002) 157;  
(c) J. Gao, S.H. Zhong, R.A. Zingaro, *J. Mol. Catal. A* 207 (2004) 15;  
(d) S.J.A. Guieu, A.M.M. Lanfredi, C. Massera, L.D. Pachón, P. Gamez, J. Reedijk, *Catal. Today* 96 (2004) 259;  
(e) M. Huisman, I.A. Koval, P. Gamez, J. Reedijk, *Inorg. Chim. Acta* 359 (2006) 1786;
- (f) S. Gupta, J.A.P.P. van Dijk, P. Gamez, G. Challa, J. Reedijk, *Appl. Catal. A* 319 (2007) 163.
- [8] (a) A.S. Hay, *J. Polym. Sci. A* 36 (1998) 505;  
(b) H. Higashimura, K. Fujisawa, M. Kubota, S. Kobayashi, *J. Polym. Sci. A: Polym. Chem.* 43 (2005) 1955.
- [9] (a) G.D. Staffin, C.C. Price, *J. Am. Chem. Soc.* 82 (1960) 3632;  
(b) C.C. Price, N.S. Chu, *J. Polym. Sci.* 61 (1962) 135.
- [10] (a) H. Komoto, K. Ohmura, *Makromol. Chem.* 166 (1973) 57;  
(b) V. Percec, T.D. Shaffer, *J. Polym. Sci., Polym. Lett. Ed.* 24 (1986) 439;  
(c) K. Muhlbach, V. Percec, *J. Polym. Sci., Polym. Chem. Ed.* 25 (1987) 2605.
- [11] (a) R. Ikeda, J. Sugihara, H. Uyama, S. Kobayashi, *Macromolecules* 29 (1996) 8702;  
(b) Y.M. Chung, W.S. Ahn, P.K. Lim, *J. Mol. Catal. A* 148 (1999) 117.
- [12] P. Gamez, J.A.P.P. van Dijk, W.L. Driessen, G. Challa, J. Reedijk, *Adv. Synth. Catal.* 344 (2002) 890.
- [13] (a) N. Eghbali, C.J. Li, *Green Chem.* 9 (2007) 213;  
(b) S. Sharma, B. Kerler, B. Subramaniam, A.S. Borovik, *Green Chem.* 8 (2006) 972.
- [14] M. Matsushita, K. Kamata, K. Yamaguchi, N. Mizuno, *J. Am. Chem. Soc.* 127 (2005) 6632.
- [15] K. Saito, T. Tago, T. Masuyama, H. Nishide, *Angew. Chem., Int. Ed.* 43 (2004) 730.
- [16] S. Mukhopadhyay, P.B. Chatterjee, D. Mandal, G. Mostafa, A. Caneschi, J. van Slageren, T.J.R. Weakley, M. Chaudhury, *Inorg. Chem.* 43 (2004) 3413.
- [17] H.Y. Han, S.J. Zhang, H.W. Hou, Y.T. Fan, *Eur. J. Inorg. Chem.* (2006) 1594.
- [18] H.Y. Han, Y.L. Song, H.W. Hou, Y.T. Fan, Y. Zhu, *Dalton Trans.* (2006) 1972.
- [19] A.C. Campos, A.G.S. Zafra, J.M.G. Pérez, J.N. Gutiérrez, E. Chinea, A. Mederos, *Inorg. Chim. Acta* 241 (1996) 39.
- [20] A. Castiñeiras, J.M. Tercero, A. Matilla, J.M. González, A.G. Sicilia, J. Niclós, *J. Coord. Chem.* 35 (1995) 61.
- [21] G. Aromí, P. Gamez, H. Kooijman, A.L. Spek, W.L. Driessen, J. Reedijk, *Eur. J. Inorg. Chem.* (2003) 1394.
- [22] P.J. Baesjou, W.L. Driessen, G. Challa, J. Reedijk, *J. Mol. Catal. A* 110 (1996) 195.
- [23] F.J. Viersen, G. Challa, J. Reedijk, *Recl. Trav. Chim. Pays-Bas* 109 (1990) 97.
- [24] M. Hassanein, F.I. Abdel-Hay, T.E. El-Esawy, *Eur. Polym. J.* 30 (1994) 335.
- [25] B. Xiao, H.W. Hou, Y.T. Fan, *J. Organomet. Chem.* 692 (2007) 2014.
- [26] (a) P. Gamez, C. Simons, R. Steensma, W.L. Driessen, G. Challa, J. Reedijk, *Eur. Polym. J.* 37 (2001) 1293;  
(b) S. Tanase, P.M. Gallego, E. Bouwman, G.J. Long, L. Rebbouh, F. Grandjean, R. Gelder, I. Mutikainen, U. Turpeinen, J. Reedijk, *Dalton Trans.* (2006) 1675.
- [27] X.R. Meng, Y.L. Song, H.W. Hou, H.Y. Han, B. Xiao, Y.T. Fan, Y. Zhu, *Inorg. Chem.* 43 (2004) 3528.
- [28] X.J. Xie, G.S. Yang, L. Cheng, F. Wang, *Huaxue Shiji* 22 (2000) 222.
- [29] G.M. Sheldrick, *SHELXL-97*, Program for Refinement of Crystal Structure, University of Göttingen, Germany, 1997.